Journal of Applied Science and Environmental Studies
JASES
http://revues.imist.ma/index.php?journal=jases

Tridentate pyrazole compounds: Synthesis, characterization and catalytic study of phenoxazinone synthase with DFT study

H. allali[1], Y. kaddouri[1], El. Yousfi[2], M. El Kodadi [1,3*], And R. Touzani[1]

[1] *Laboratory of Applied and Environmental Chemistry, Mohammed first University, Oujda, Morocco.*
[2] *Higher Institute of Nursing and Health Professions techniques, Oujda, Morocco.*
[3] *CRMEF Oriental, Centre Régional des Métiers de l'Education et de Formation Oujda, Morocco.*

Received 9 Jan 2019 ; Revised 20 Jan 2019, Accepted 21 Feb 2019

**Corespondance authors : elkodadim@yahoo.fr*

Keywords
Phenoxazinone,
Pyrazole,
Tridentate,
Synthase,
Catalysis.

Abstract
Thepyrazole derivatives are the subject of various studies and used in many different fields, such as pharmacology, biology and catalysis. In this work we will focus on the synthesis of new pyrazole tridentate ligands to prepare catalysts to replicate the catalytic activity of ortho-aminophenol. We have studied the catalytic activity of oxidation of ortho-aminophenol to phenoxazinone by using complexes formed in situ, by mixing tridentate pyrazole ligands with manganese (II) chloride. Then using DFT method to have more information's about the reactivity of the prepared ligands, The results shows that T_7 is the best electron donor, T_6 is the most reactive ligand with the lowest value of gap energy, and T_5 with the lowest value of the hardness is assigned with the ability for it to give or accept electron.

1. Introduction

Pyrazoles are among the most studied heterocyclic aromatic compounds, acting both as simple ligands and incorporated into tridentate ligands. Pyrazole derivatives are the subject of various studies and are used in many different fields, such as pharmacology [1, 2], biology, electronics [3]. and catalysis[4-7]. They have catalytic, anticonvulsant [8], antifungal activity [9], antihistamine [10], antidepressant [11] and anti-stress [12], antitumor [13] as well as anti-cancer properties, pharmacological activities and other therapeutic action spectrum of diseases. This evolution is reflected by an exponential increase of the number of publications, which refer to these compounds. Among the numerous molecular structures discovered, several pyrazole skeletons have been synthesized in this domain [14, 15]. The

pyrazole derivatives, which are well known for their ability to complex and transport the transition and alkali metal cations. These compounds are characterized by the presence of several substituted pyrazole rings linked together through different substituents, which can considerably affect their complexing [16], corrosion inhibiting [17], catalytic properties [6, 18] as well as their cytotoxic activities [19] and antifungal agents and lack antibacterial activity [20]. The researchers in our laboratory synthetized many pyrazole derivatives to investigate their properties [21-27].

Several studies have been carried out on the mechanism and kinetics of the catalytic oxidation of phenoxazinone synthase of 2-aminophenols by complexes of metals (Mn, Co and Cu) [28-43] as functional models catalyzed the oxidation reaction of the o -aminophenol to phenoxazinone synthase in the presence of dioxygen.

These new synthesized heterocyclic systems are likely to be endowed with visible biological activity or used as ligands in the synthesis of new complexes based on transition metals given the existing two nitrogens on the pyrazole backbone with the following properties, electron-rich compounds (donors from 6 to 12 electrons), high diversity by the possibility of different substituents and flexible junction (N-C-N).In this work we are concerned with the synthesis and characterization of pyrazolic tridentate compounds, manganese complexes and catalytic oxidation study of o-aminophenol in the presence of complexes prepared in situ based on tridentate pyrazole ligands and manganese (II) chloride.

In this study we initiated theoretical investigations using DFT [44] method with B3LYP basis 6-31G (d,p) which is widely used to study the reactivity of the ligands by calculating many quantum parameters like: E_{gap}, E_{HOMO}, E_{LUMO} and Dipolar moment, other than the ones resulted after the calculations using GAUSSIAN09W [45] which are the ionization energy, the electronic affinity and the hardness.

2. Materials and Methods

2.1. Synthesis

The starting precursors 1-hydroxymethyl-3,5-dimethylpyrazole L_1, 1-hydroxymethyl-pyrazole L_2 and 1-hydroxymethyl-3-methyl-5-esterpyrazol L_3 were prepared according to the method described in literature [46] by condensation of 3,5-dimethylpyrazole, 1H-pyrazole and 3-methyl-5-esterpyrazole with formaldehyde in aqueous solution respectively (Scheme 1).

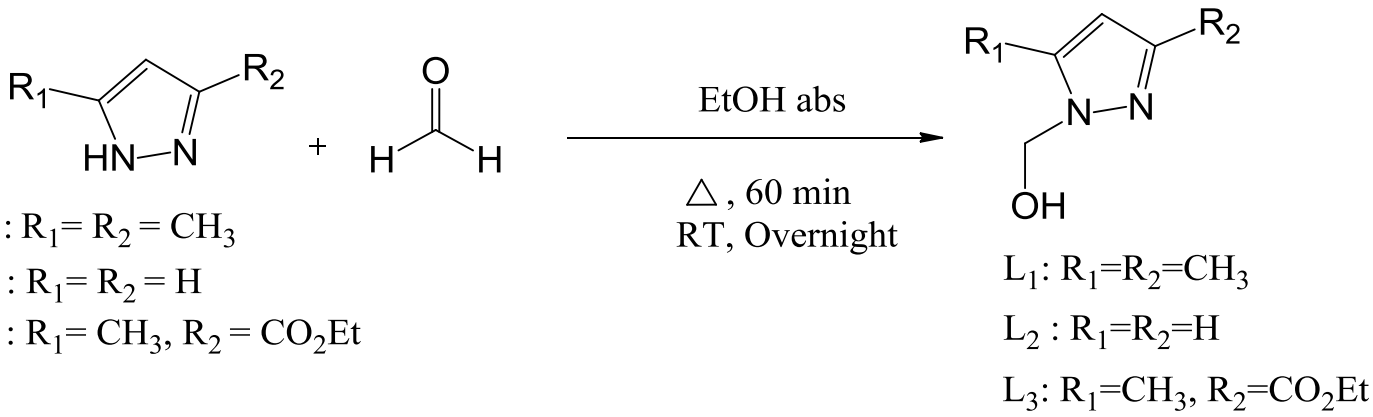

a : $R_1 = R_2 = CH_3$

b : $R_1 = R_2 = H$

c : $R_1 = CH_3$, $R_2 = CO_2Et$

L_1: $R_1 = R_2 = CH_3$

L_2 : $R_1 = R_2 = H$

L_3: $R_1 = CH_3$, $R_2 = CO_2Et$

Scheme1 : Method of synthesis of compounds L_1, L_2 and L_3

2.2. Synthesis of tridentate products based on pyrazole T_1-T_7

The synthesis strategy of the **T_1-T_7**dialkylation structures is essentially based on the creation of the NCN junction bonds by a twoequivalent condensation reaction of 1-hydroxymethyl-3,5-dimethylpyrazole **L_1**, 1-hydroxymethyl-pyrazole **L_2** and 3-methyl 5-esterpyrazole **L_3**, with the various primary amines heated to reflux of acetonitrile for 4h, it is reported that the **T_1-T_7**compounds are already described in the literature [47-49] (Scheme2).

The tridentate ligands are characterized **T_1-T_7**by IR and UV-visible and H^1NMR, the infrared spectra ofthe samples were recorded in the range of 500–4000 cm^{-1}on aPerkinElmer Spectrum Two Infrared spectrometer using KBrpel-lets. The UV-visible adsorption spectra of the **T_1-T_7**compounds in methanol ($C = 10^{-4}$ M) are characterized by the presence of about one band (290 nm, 332 nm), observed in the ultraviolet range figure 1. The intraligand transitions π-π*, n-π* which involve the ligand alone. These products have also shown good absorption and sometimes a continuous way in the UV region, which also allows us to consider their use as U.V radiation absorbers. The H^1 NMR spectrum was recorded at room temperature on a 600 MHz Bruker apparatus at MASIR, Rabat, Morocco.

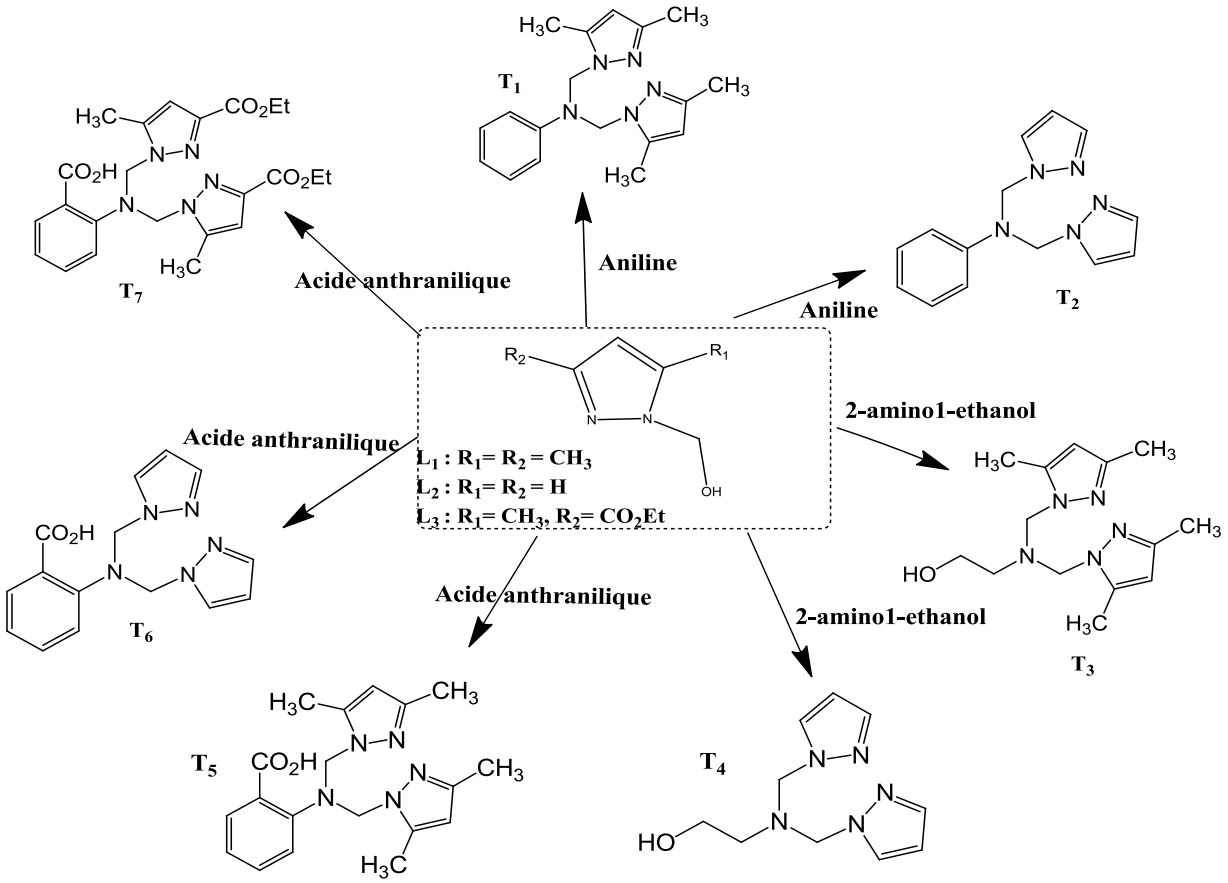

Schema 2 : Structure of pyrazolic tridentate products T_1-T_7

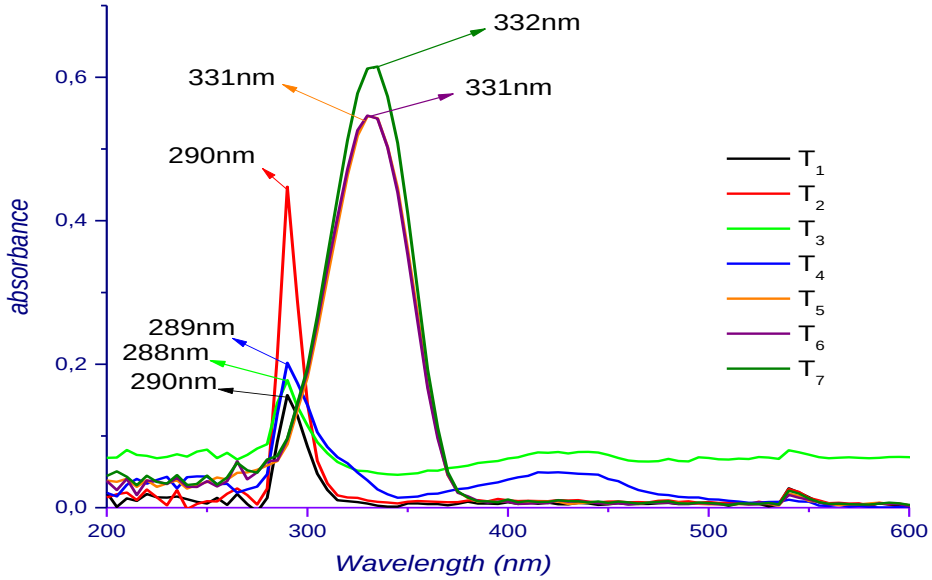

Figure 1 : UV-Visible absorption spectra of ligands **T_1-T_7** in methanol

T_1 :Appearance: Solid salmon color,Yield = 84%, Mp: (68-70)°C, FTIR: (KBr, v (cm^{-1}): 3294(C-H_{tri}-aro); 2915; 1606(C=N); 1548(C=C); 1507; 1208 and 1262(C-N); 751(C-$H_{aromati}$).UV-Visible (CH_3OH; λmax, nm(ε, l/mol/cm)): 290(1498.680).

T_2 :Appearance: Viscous red garnet color,Yield =67%. FTIR: (KBr, v (cm^{-1}): 3427-3314; 3110(C-H); 2956; 1604(C=N); 1504; 1050(C-N); 756. UV-Visible (CH_3OH; λmax, nm(ε, l/mol/cm)): 290(4462.777).

T_3 :Appearance: Beige solid color,Yield =74%, Mp: 74-76 °C. FTIR: (KBr, v (cm^{-1}): 3458-3151(C-H_{arom}); 2931-2859(OH); 1553; 1032(C-N); 784. UV-Visible (CH_3OH; λmax, nm(ε, l/mol/cm)): 288(17629.356).

T_4 :Appearance: Yellow viscous,Yield =64%. FTIR: (KBr, v (cm^{-1}): 3360(OH); 3120(CH); 2961-2874; 1517(C=C); 1400; 1050(O-CH_2); 761.UV-Visible (CH_3OH; λmax, nm(ε, l/mol/cm)): 289(19846.885).

T_5 :Appearance: White solid,Yield =59%, Mp: 140-142°C. FTIR: (KBr, v (cm^{-1}): 3852; 3739; 3345; 2353(OH_{acide}); 1670(C=O); 1522(C=C); 1218(C-N); 749($CH_{aromat;o\text{-}disbs}$).UV-Visible ($CH_3OH$; λmax, nm(ε, l/mol/cm)): 331(5414.467).RMN^{1}H (DMSO-d_6)δ_{ppm} : 5.17(d, 1H, HC=CH-CH); 5.47(s, 2H, N-CH_2-N); 5.88(s, 2H, N-CH_2-N); 7.50-7.41(m, 5H); 6.29-6.22(m, 3H).

T_6 :Appearance: White solid,Yield =54%, Mp: 78-80°C. IR: (KBr, v (cm^{-1}): 3360(OH_{acide}); 3115(CH); 1711(C=O); 1655(C=N); 1221(C-N); 743($CH_{aromat;o\text{-}disbs}$).UV-Visible ($CH_3OH$; λmax, nm(ε, l/mol/cm)): 331(5436.642). RMN^{1}H (DMSO-d_6)δ_{ppm} : 2.09 (m, 3H, $PzCH_3$); 2.26 (d, 3H, $PzCH_3$); 5.17 (d, 2H, J=3.7Hz); 5.81 (d, 3H, J=14.8Hz); 8.68 (s, 1H, OH_{acide}).

T_7 :Appearance: White solid,Yield =52%, Mp: 156-158°C. FTIR: (KBr, v (cm^{-1}): 3355(OH_{acide}); 1721(C=O); 1675(C=C); 1520; 1213(C-N); 746($CH_{aromat;o\text{-}disbs}$). UV-Visible ($CH_3OH$; λmax, nm(ε, l/mol/cm)): 332(6100.053).

2.3. Synthesis and characterization of complexes based on tridentate ligands

The manganese complex (C_1-C_3) was prepared by adding a solution of the tridentate ligand (T_2, T_6 and T_7)

(1mmol) in methanol (3 ml) to a solution of hydrated manganese salt (II) ($MnCl_2$, $4H_2O$) (1 mmol) in methanol (3 ml)). The reaction mixture is heated at reflux for one hour. The resulting solution is filtered and left at 20°C, and then washed with a little methanol. The general coordination reaction of the ligands with manganese is shown in Scheme3. The complexes formed are characterized by IR and UV-Visible.

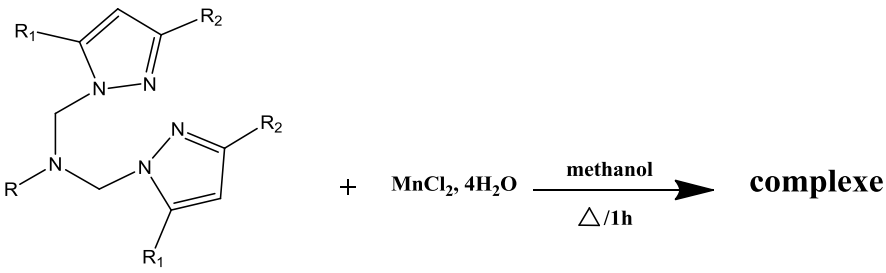

T_2 R = Aniline $R_1 = R_2 = H$ **C1**

T_6 R = acide anthranilique $R_1 = R_2 = H$ **C2**

T_7 R = acide anthranilique $R_1 = CH_3$, $R_2 = CO_2Et$ **C3**

Scheme 3 : The general coordination reaction of ligands with manganesechlorid

The figure below (figure 2) gathers the spectra of the prepared complexes. Solutions of manganese (II) chloride absorb both visible and UV regions. The visible transitions are of type d-d and have a very low intensity.

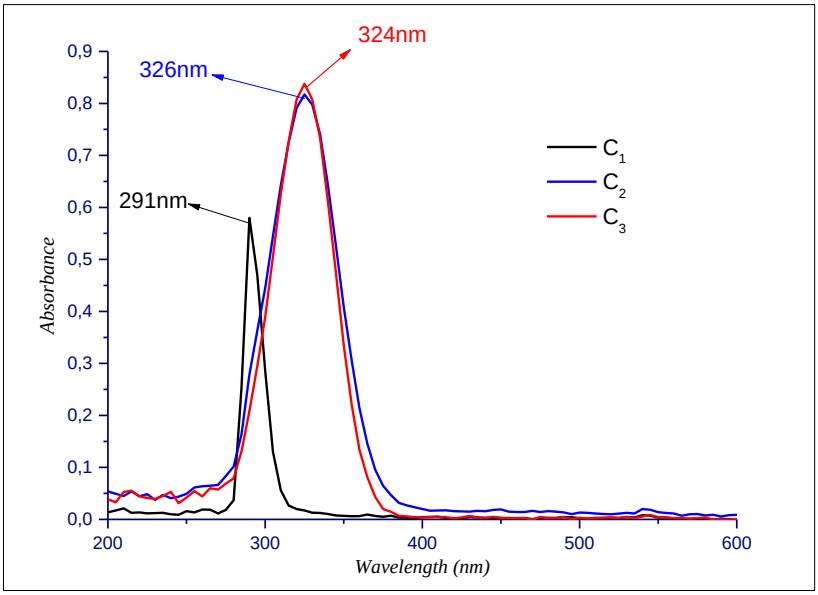

Figure2 : UV.Visible absorption spectra of (**T_2**, **T_6** and**T_7**) based manganese chloridcomplexes

Complexe**C_1**: Appearance: Solid salmon color, Mp(°C) :176-178, FTIR (KBr, ν(cm^{-1})): 3514(OH); 3374(H_2O); 3120(=CH); 1614(C=N); 1512; 1106(C-N); 746($CH_{aromatique(ortho)}$). UV-Visible (CH_3OH; λmax, nm(ε, l/mol/cm)): 291(291.236).

Complexe**C**$_2$: Appearance: solid red color, Mp(°C): 164-166, IR (KBr, ν(cm^{-1})): 3360(OH$_{acide}$); 1665(-C=O$_{acide}$); 1591(C=N); 1218(C-N); 754(CH$_{aromatique}$).UV-Visible (CH$_3$OH; λmax, nm(ε, l/mol/cm)): 326(406.264).

Complexe**C**$_3$:Appearance: Solid yellow, Mp(°C): 160-162.FTIR (KBr, ν(cm^{-1})): 3499(H2O); 3355(OH); 1724(-C=O); 1683(-C=O$_{acide}$); 1586(C=C); 1520(C=C); 1213(C-N); 746(CH$_{aromatique(ortho)}$). UV-Visible (CH$_3$OH; λmax, nm(ε, l/mol/cm)): 324(415.365).

3. Results and Discussion

3.1.Kinetics of the phenoxazinone synthase activity

Kinetic study of synthase of o-aminophenol to phenoxazinone in the presence of complexes prepared in situ based on tridentate ligands **T$_1$-T$_7$**. The oxidation of o-aminophenol to phenoxazinone is according to the reaction (scheme 4):

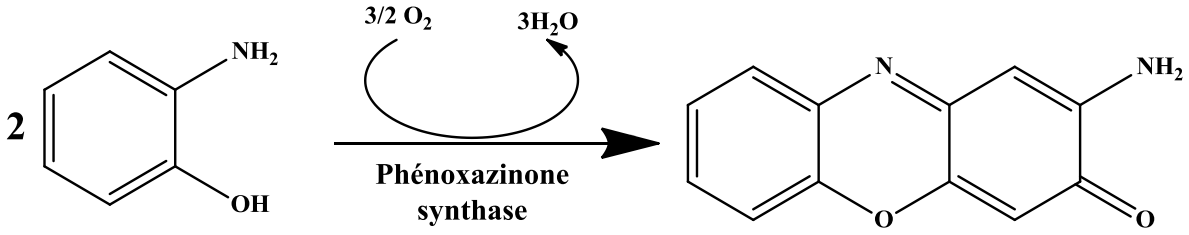

O-Aminophénol(OAPH) **2-Aminophénoxazinone-3-one (APX)**

Scheme 4 : Reaction scheme of phenoxazinonesynthase

The kinetic measurements were performed on a Jenway UV-visible spectrophotometer in the ISPITSO laboratory following phenoxazinone formation as a function of time at room temperature. The characteristic band of phenoxazinone at 435 nm was used to follow the reaction of the substrate synthase. The different kinetic parameters were determined by the initial velocity method.

3.2. Study of the catalytic activity of manganese (II) complexes based on T$_1$-T$_7$ligands prepared in situ

In this study, the complex is prepared in situ by mixing 0.15 ml of a 2 × 10^{-3}mol / l solution of ligand (**T$_1$-T$_7$**) dissolved in methanol and 0.15 ml of a solution of the manganese salt $MnCl_2$. The mixture is allowed to stand for about 10 minutes and then 2 ml of a 10^{-1}mol / l solution of o-aminophenol is added. After the addition, the formation of phenoxazinone is followed by the evolution of the absorbance

at 435 nm as a function of time after adjustment to zero, the experiments are carried out at room temperature.The measurements of the evolution of the absorbance as a function of time are given in figure 3 and the oxidation rates of the complexes obtained are collated in table 1.

As can be seen, the results reveal that all complexes showed activity towards the oxidation of o-aminophenol to phenoxazinone. But with different activity which vary from 3.78 µmol. mg^{-1}. min^{-1} for the complex arising from pyrazole ligand **T_7**as is weak catalyst to 31.26 µmol.mg^{-1}.min^{-1} for the complex formed from ligand **T_4**and the manganese salt as is best catalyst with a turnover equal to 10846.58 min^{-1}.

Table 1 : Catalyticparameters of complexes based on T_1-T_7 ligands

ligands	V(µmol/mL/min)	a(µmol/mg/min)	T(min^{-1})
T_1	2.61	22.98	10004.07
T_2	2.62	26.50	10048.66
T_3	2.90	27.52	11097.58
T_4	2.83	31.26	10846.58
T_5	2.67	21.38	10245.99
T_6	2.63	23.80	10070.80
T_7	0.59	3.78	2251.68

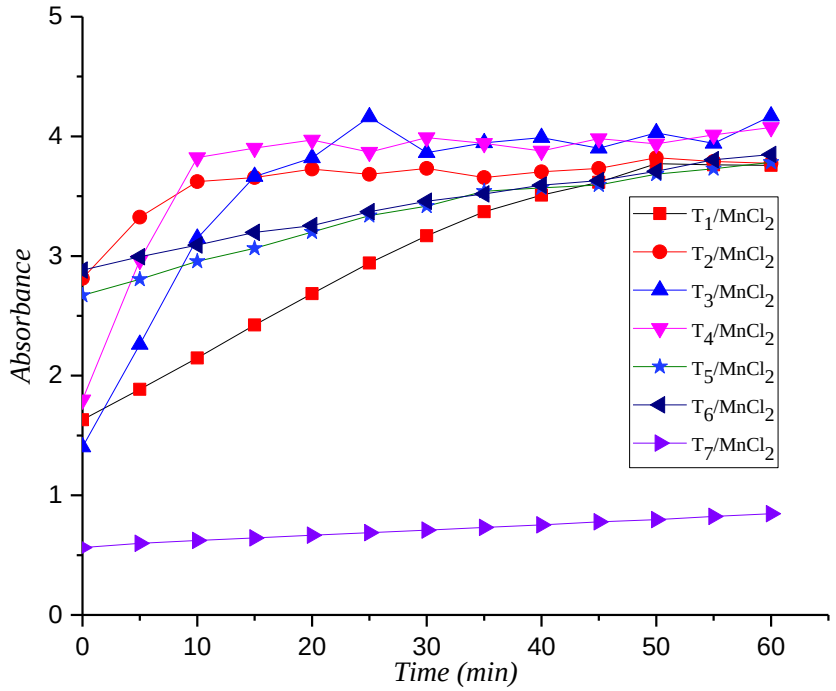

Figure 3 : Oxidation of o-aminophenol in the presence of complexes formed by ligands (T_1-T_7)

3.3. Kinetic study

To determine the K_m and V_m constants of the oxidation reaction of o-aminophenol in a solvent (methanol), the Michaelis curve (Vi = f (o-aminophenol) five ligands was used. The first method consists of plot the graph of Vi versus substrate concentration "o-aminophenol" (figures4-7). This study carried out for the complexes prepared in situ as follows: ($T_1/MnCl_2$), ($T_3/MnCl_2$), ($T_4/MnCl_2$), ($T_5/MnCl_2$) and ($\mathbf{T_6}/MnCl_2$) will allow to determine the concentration of o-aminophenol which gives the maximum speed under the conditions of study. The experiment is carried out by mixing 0.15mL of a solution of 2×10^{-3}mol/Lof ligands (**T_1**, **T_3-T_6**) and 0.15mL of a solution of the manganese salt $MnCl_2$ of 2×10^{-3}mol/L. The mixture is allowed to stand for about 10 minutes and then 2 ml of a solution of o-aminophenol at an alternating concentration of 10^{-3}mol/L at 0.8 mol/L in a spectrophotometric cell at 25°C. is added and the measurement is carried out. absorbance of phenoxazinone formed as a function of time. The figures below show the measurements made. Table 2 summarizes the different activity parameters (V_m and K_m) for these five complexes.

Table 2: Maximum rate (V_m) and rate constants (K_m) of the five combinations**Ti**/$MnCl_2$.

Ligands/salt	V_m(µmol/mL/min)	K_m (mol. L^{-1})
$T_1/MnCl_2$	5.29	0.0408
$T_3/MnCl_2$	4.66	0.1060
$T_4/MnCl_2$	4.46	0.0586
$T_5/MnCl_2$	4.44	0.0609
$T_6/MnCl_2$	4.49	0.0632

For the various complexes prepared in situ, the formation rates of phenoxazinone increase with the concentration of o-aminophenol, but almost from the concentration 0.1 mol/L, the increase of the speed becomes low then we arrive at the maximum speed. We thus determined the various parameters: The K_m rate constant and the oxidation rate V_m of o-aminophenol to phenoxazinone for each complex formed in situ (table 2). These rateV_m are similar for the various complexes with a slight increase for the **T_1** and **T_3** ligand-based complexes, the T_1 ligand is characterized by a maximum rate of 5.29µmol $L^{-1}min^{-1}$ and a rate constant K_m is smaller equal to 0.0408 mol.L^{-1}.

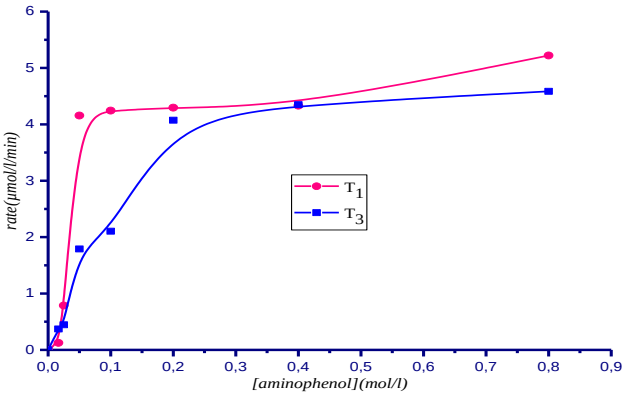

Figure 4 : Dependence of the reaction rates on the aminophenol concentrations for the oxidation reaction catalyzed by complex arising from T_1 and T_3 with $MnCl_2$ in methanol

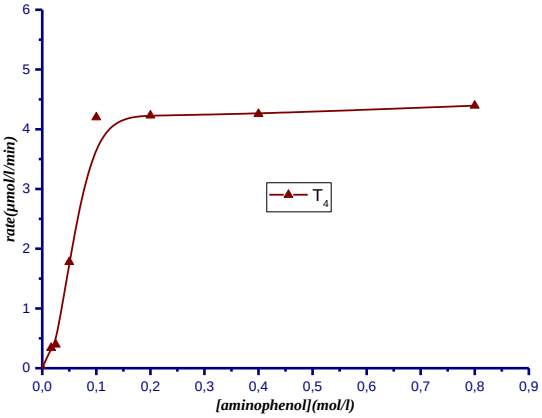

Figure 5 : Dependence of the reaction rates on the aminophenol concentrations for the oxidation reaction catalyzed by complex arising from T_4 with $MnCl_2$ in methanol

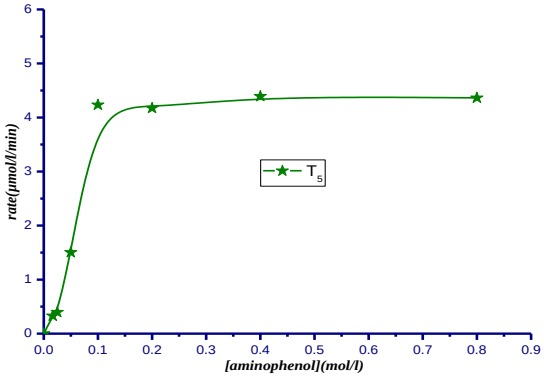

Figure 6 : Dependence of the reaction rates on the aminophenol concentrations for the oxidation reaction catalyzed by complex arising from T_5 with $MnCl_2$ in methanol

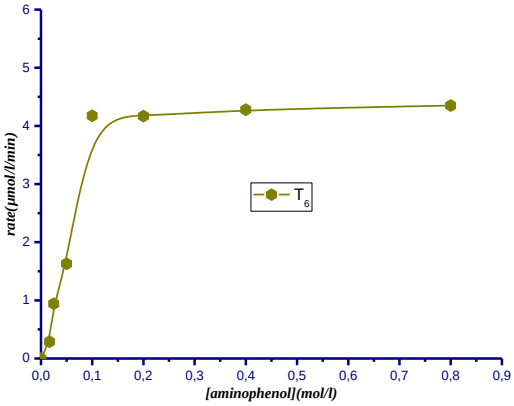

Figure 7 : Dependence of the reaction rates on the aminophenol concentrations for the oxidation reaction catalyzed by complex arising from T_6 with $MnCl_2$ in methanol

3.4. UV-Vis spectrophotometric study

To confirm the important catalytic activity for the **T_5**/$MnCl_2$ and**T_6**/$MnCl_2$ combinations, phenoxazinone formation kinetics were recorded in every 5 min. The kinetic experiments were performedat room temperature. The figure 8 clearly show the appearance of a concentrated band at 435 nm, which explains why all combinations are able to easily catalyze the oxidation of o-aminophenol to phenoxazinone.

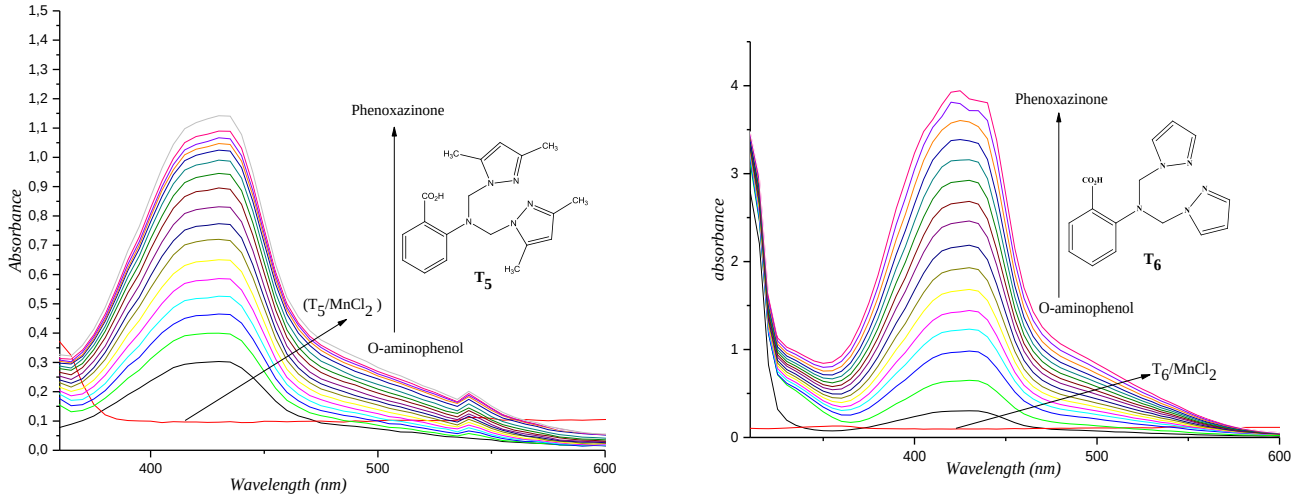

Figure 8. Increase of phenoxazinone band at 435 nm after addition of the o-aminophenol solution (2mL, 10-1mol.L-1) to a solution containing ligand **T_5** or **T_6** (*0.15mL, 2x10-3 mol.L^{-1}) and $MnCl_2$ (0.15mL, 2x10-3 mol.L-1) in methanol. The spectra were recorded after every 10 min.*

3.5. Proposed Reaction Pathway.

The mechanism of the reaction is based mainly on an earlier proposal derived from spectroscopy and theoretical studies [50,51]. We try to present an oxidation mechanism of o-aminophenol, according to the figure 9, the mechanism of synthase activity (outer circle) starts from the complex.

3.6. DFT Study

The DFT study was executed on Dell OptiPlex 790 MT – Core i5-2400 @ 3,10Ghz with 4 Gb RAM and an operating system: Windows 7 Pro 64 Bits. First the Full geometry optimizations of the ligands have been performed using Gaussian 09W software [45] with B3LYP exchange correlation [44,53,54] in combination with 6-31G (d, p) orbital basis sets for all atoms, and no symmetry constrains were applied.

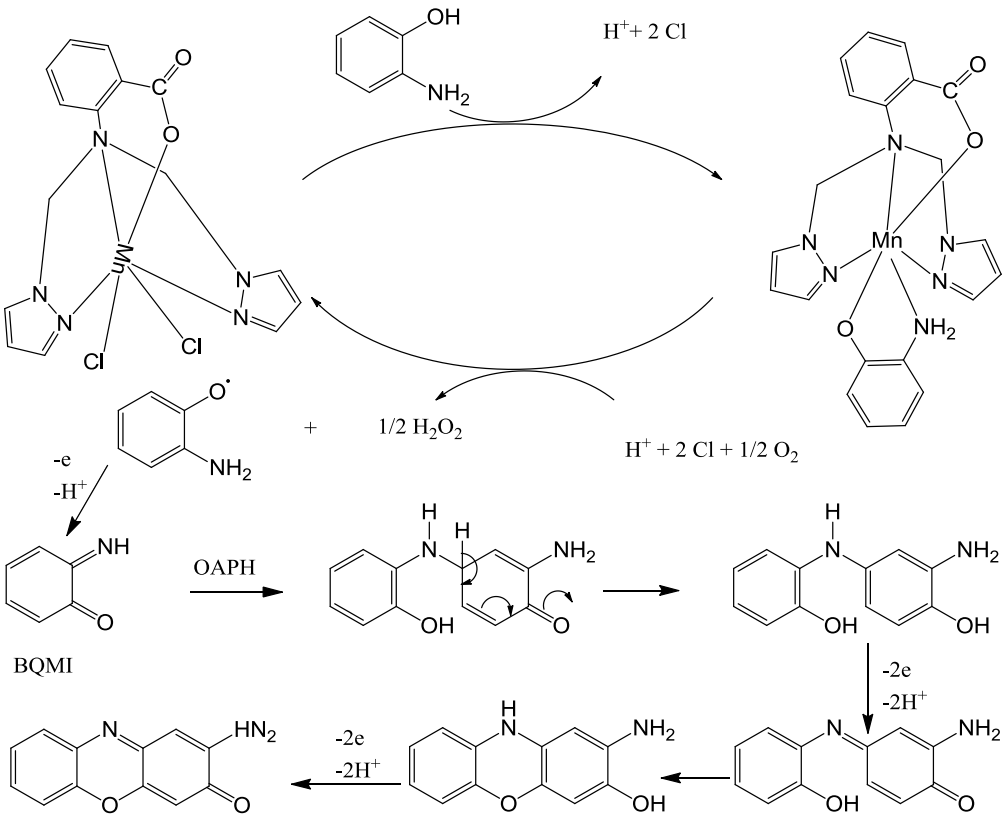

Figure 9 : *Proposed mechanism for phenoxazinone formation [52]*

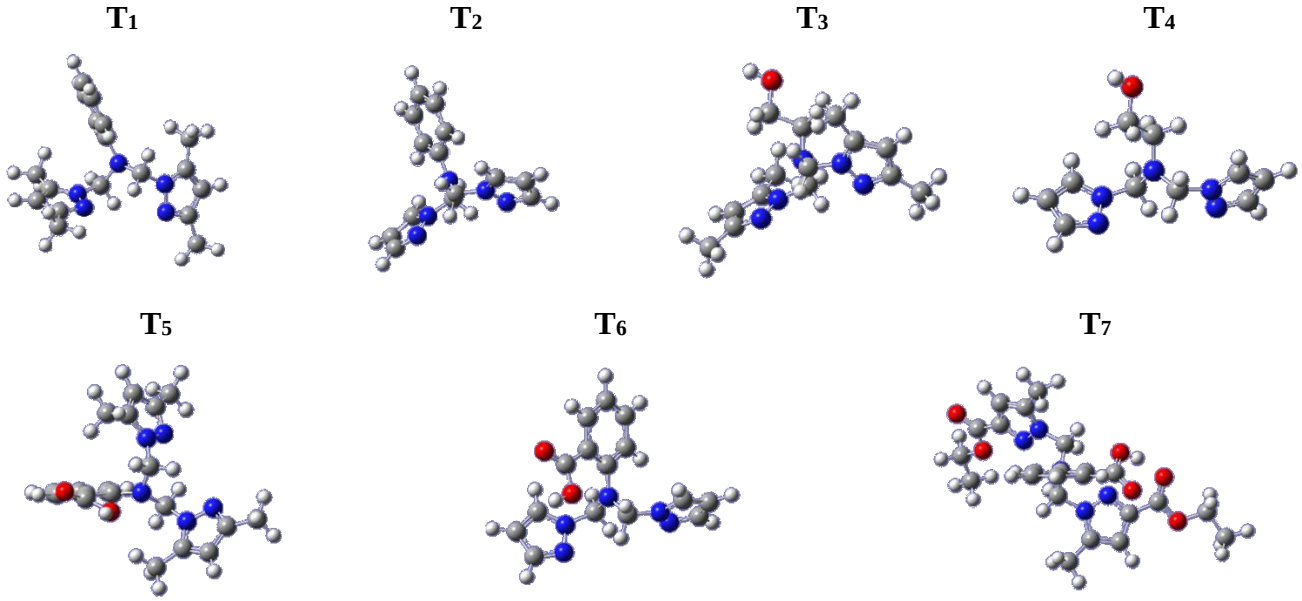

Figure 10.*Geometrical optimized structures of the ligands* ***T₁-T₇***

For the quantum descriptors, we found in the results after the calculation is done only E_{HOMO}, E_{LUMO} andwe calculated using the following equations:

$$\Delta E_{gap} = |E_{HOMO} - E_{LUMO}| \quad (1)$$

By Koopmans theory [56], we have:

$$I = -E_{HOMO} \ (2); A = -E_{LUMO} \ (3) \text{and} \ \eta = \frac{I - A}{2} \ (4)$$

Table 3. *The quantum descriptors values founded and calculated for the ligands* ***T_1-T_7***

	E_{HOMO} (eV)	E_{LUMO} (eV)	ΔE_{gap}(eV)	I (eV)	A (eV)	η (eV)
T_1	-5,6942	-0,2008	5.4934	5,6942	0,2008	2,7467
T_2	-5,6362	-0,0419	5.5943	5,6362	0,0419	2,7972
T_3	-5,8539	0,6443	6.4982	5,8539	-0,6443	3,2491
T_4	-6,1195	0,4908	6.6103	6,1195	-0,4908	3,3052
T_5	-5,8621	-3,0585	2.8036	5,8621	3,0585	1,4018
T_6	-6,1685	-1,4487	4.7198	6,1685	1,4487	2,3599
T_7	-6,3282	-0.0354	6.2927	6,3282	0.0354	3,1464

From the data in table 3, we retrieve the following information:

HOMO or the highest occupied molecular orbital (in energy) is the easiest orbital to give electron and LUMO or the lowest unoccupied molecular orbital (in energy) is the easiest orbital to accept electron, for our study it's the case of T_7 due the presence of the methyl with ester on the Pyrazole ring and the acidic function on the aromatic ring which make a conjugation on the bunds.

The gap energy is another important quantum descriptor [55] which represents the gap between HOMO and LUMO orbitals (in energy) so the necessary energy to do the first excitation of the ligand, so T_6 is the most reactive ligand between all of the studied ligands.

The hardness (**η**) reflects the ability of the ligand to resist faces to electron number change. The lowest value of it is assigned with the ability to give or accept electron which is the case of **T_5**.

For the Frontier molecular orbitals of the ligands, we used the same described parameters for the DFT study, and it's very important to have an idea about the different sites in the ligand.

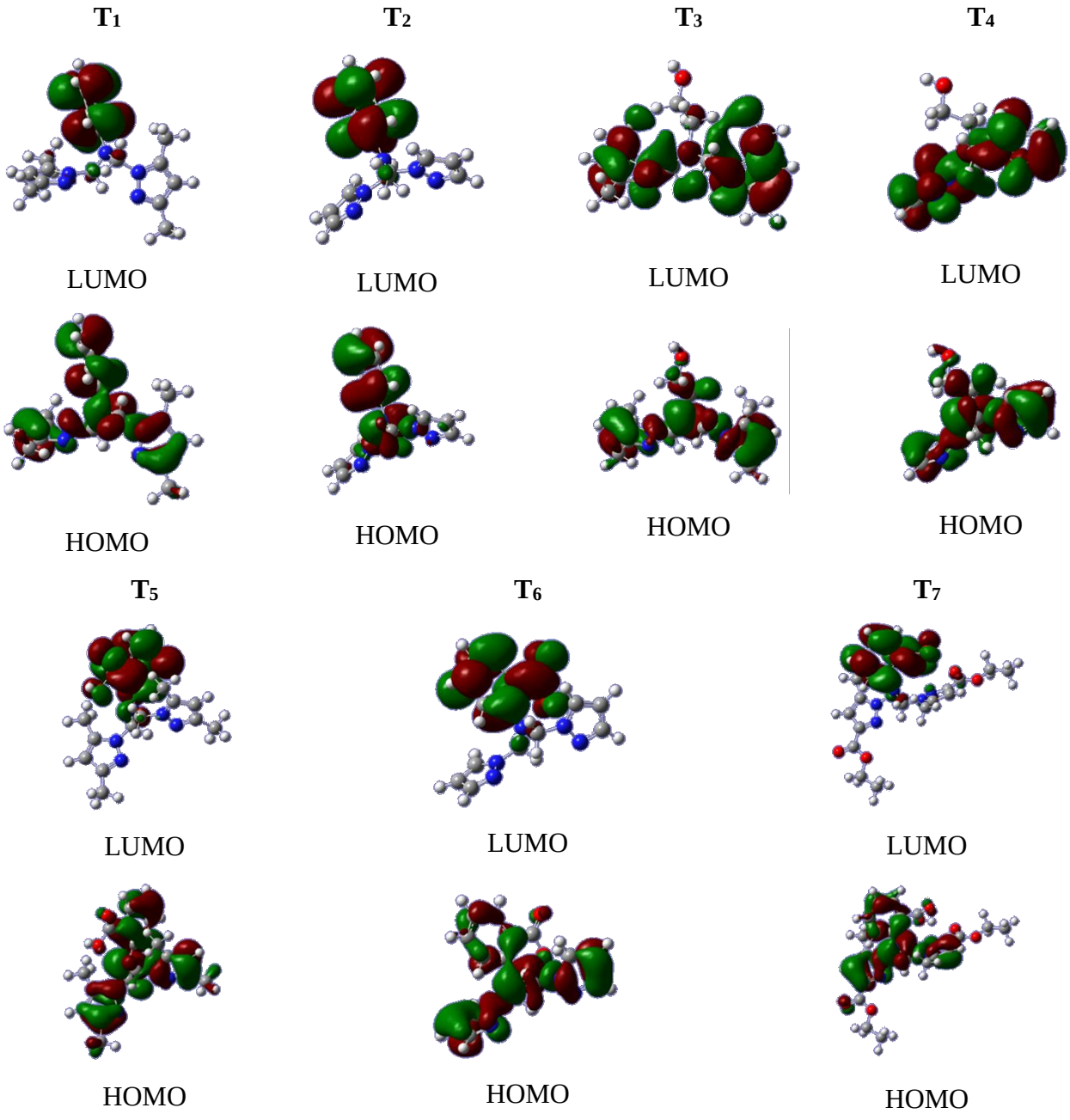

Figure 11 : *Frontier molecularOrbitals of* ***T_1-T_7***

Conclusion

In this study we have described the reproduction of the catalytic activity of o-aminophenol synthase by employing manganese complexes which have formed in situ, by mixing ligands and manganese chloride. The results obtained show that all the complexes catalyze the oxidation of o-aminophenol to phenoxazinone. And to better understand the parameters influencing the catalytic activity of the complexes studied which controlled the o-aminophenol synthase activity of the systems studied.Growth of the adsorption peak at 435 nm, characteristic of the chromophoricphenoxazinone, was observed, indicating a catalytic oxidation of o-aminophenol to phenoxazinone. The time-dependent spectral profiles over a period of 2h after the addition of o-aminophenol, for the complexes prepared in situ **T5**/$MnCl_2$, **T6**/$MnCl_2$ and **T7**/$MnCl_2$. A control experiment was conducted using manganese (II) chloride in place of the complexes formed, and this shows no increase significance of the intensity of the band at 435 nm under identical reaction conditions. These observations may account for how all complexes exhibit phenoxazinone-like activity at synthase under aerobic conditions.

From the theoretical investigations using DFT method, we have that T_7 is the best electron donor between all the ligands due to the presence of the methyl with ester on the Pyrazole ring and the acidic function on the aromatic ring which make a conjugation on the bunds, T_6 is the most reactive ligand between all of the studied ligands because of it lowest value of gap Energy, and T_5 with the lowest value of the hardness is assigned with the ability for it to give or accept electron.

References

1. F. Malek, N. Draoui, O. Feron, S. Radi, Res. Chem. Intermed, 40(2) (2014) 681-687.
2. T. Harit, F. Malek, B. El Bali, A. Khan, K. Dalvandi, B. P. Marasini, S. Noreen, R. Malik, S. Khan, M. I. Choudhary, Medicinal Chemistry Research, 21(10) (2012) 2772-2778.
3. A. G. Zavozin, N. V. Ignat'ev, M. Schulte, M. S. G. Zlotin, Tetrahedron 71(45) (2015) 8551-8556.
4. M. El Kodadi, F. Malek, R. Touzani, A. Ramdani, Catal. Commun. 9(5) (2008) 966-969.
5. R. Boyaala, R. El Ati, F. Abrigach, M. El Kodadi, R. Touzani, and B. Hammouti, RJPBCS 8(3), 2017.
6. R. Boyaala, R. El Ati, M. Khoutoul, M. El Kodadi, R. Touzani and B. Hammouti, J. Iran. Chem. Soc, 2018, 15(1), 85–92.
7. H. Y. Ding, H. J. Cheng, F. Wang, D. X. Liu, H. X. Li , Y. Y. Fang, W. Zhao, J. P. Lang, J. Organomet. Chem.741-742(2013) 1-6.
8. V. Michon,C. Hervé du Penhoat, F. Tombret,JM. Gillardin, F. Lepage, L. Berthon, European Journal of Medicinal Chemistry, 30(2) (1995) 147-155.
9. C. K. Chu, S. J. Cutler, Journal of Heterocyclic Chemistry, 23(2) (1986) 289-319.

10. İ. Yıldırım, N. Özdemir, Y. Akçamur, M. Dinçer, O. Andaç, ActaCrystallographica Section E, 61(2) (2005) o256-o258.
11. D. M. Bailey, P. E. Hansen, A. G. Hlavac, E. R. Baizman, J. Pearl, A. F. DeFelice, M. E. Feigenson, Journal of Medicinal Chemistry, 28(2) (1985) 256-260.
12. D. J. Wustrow, T. Capiris, R. Rubin, J. A. Knobelsdorf, H. Akunne, M. D. Davis, R. MacKenzie, T. A. Pugsley, K. T. Zoski, T. G. Heffner, . D. Wise, Bioorganic & Medicinal Chemistry Letters, 8(16) (1998) 2067-2070.
13. H. J. Park, K. Lee, S. J. Park, B. Ahn, J. C. Lee, H. Y. Cho, K. I. Lee, Bioorganic & Medicinal Chemistry Letters, 15(13) (2005) 3307-3312.
14. T. Harit, F. Malek, Sep. Purif. Technol. 176 (2017), 8-14.
15. T. Harit, R. Bellaouchi, C. Mokhtari, B. El Bali, A. Asehraou, F. Malek, Tetrahedron 73(34) (2017) 5138-5143.
16. M. Lamsayah, M. Khoutoul, A. Takfaoui, F. Abrigach, A. Oussaid, R. Touzani, Sep. Sci. Technol. 50(14) (2015) 2170-2176.
17. H. Elmsellem, T. Harit, A. Aouniti, F. Malek, A., Riahi, A. Chetouani, B. Hammouti, Prot. Metals Phys. Chem. Surfaces 51(5) (2015) 873-884.
18. Z. Bouanane,M. Bounekhel,M. Elkolli,F. Abrigach,M. Khoutoul, R. Bouyala, R. Touzani,A. Hellal, *J. Mol. Struct.*,1139(5) (2017) 238-246.
19. M. El Kodadi, M. Benamar, B. Ibrahim, A. Zyad, F. Malek, R. Touzani, A. Ramdani and A. Melhaoui, Natural Product Research, 21(11) (2007) 947-952.
20. F. Abrigach, B. Bouchal, O. Riant, Y. Macé, A. Takfaoui,S. Radi, A. Oussaid, M. Bellaoui and R. Touzani, Medicinal Chemistry, 12 (2016) 83-89.
21. V. A. Tuskaev, S. V. Zubkevich, D. Saracheno, S. Ch. Gagieva, P. V. Dorovatovskii, E. G. Kononova, V. N. Khrustalev, D. N. Zarubin, B. M. Bulychev, Y. V. Kissin, MolecularCatalysis 464 (2019) 29–38.
22. M. Behpour, S. M. Ghoreishi, N. Soltani, M. Hamadanian, and A. Gandomi, Corros. Sci., 50(8) (2008) 2172–2181.
23. M. Elayyachy, M. Elkodadi, A. Aouniti, A. Ramdani, B. Hammouti, F. Malek, A. Elidrissi, Mater. Chem. Phys., 93(2-3) (2005) 281–285.
24. K. Tebbji, H. Oudda, B. Hammouti, M. Benkaddour, M. El kodadi, F. Malek, A. Ramdani, Appl. Surf. Sci., 241(3-4) (2005) 326–334.
25. K. Sundaravel, E. Suresh, M. Palaniandavar, Inorg. Chim. Acta, 363(12) (2010) 2768–2777.
26. I. Bouabdallah, R. Touzani, I. Zidane, A. Ramdani, Catalysis Communications 8 (2007) 707–712.
27. R. Marion, M. Zaarour, N. A. Qachachi, N. M. Saleh, F. Justaud, D. Floner, O. Lavastre, F. Geneste, J. Inorg. Biochem., 105(11) (2011) 1391–1397.
28. A. Panja, M. Shyamal, A. Saha, T.K. Mandal, Dalton Trans. 43 (2014) 5443-5452.
29. A. Panja, Dalton Trans. 43 (2014) 7760-7770.
30. A. Panja, RSC Adv. 4 (2014) 37085-37094. http://dx.doi.org/10.1039/C4RA03427A
31. Bruker SAINT-plus Bruker AXS Inc., Madison, Wisconsin, USA, 2007.
32. G.M. Sheldrick, SADABS, University of Göttingen, Germany, 1996.
33. A. Panjaa, N. Ch. Jana, M. Patra, P. Brandão,C. E. Moore, D. M. Eichhorn, A. Frontera, Journal of Molecular Catalysis A: Chemical 412 (2016) 56–66.
34. A. K. Ghosh, A. Ali, Y. Singh, C. S. Purohit, R. Ghosh, Inor. Chim. Acta, 474(2018) 156-163.
35. S.Chatterjee, D. Sukul, P. Banerjee, J. Adhikar, Inorganica Chimica Acta, 474(2018) 105-112.

36. S. C. Kumar, A. K. Ghosh, J. D. Chen, R. Ghosh, Inorganica Chimica Acta, 464(2017) 49-54.
37. A. Kumar Maji, A. Chatterjee, S. Khan, B. K. Ghosh, R. Ghosh, Journal of Molecular Structure, 1146(2017) 821-827.
38. A. Hazari, A. Das, P. Mahapatra, A. Ghosh, Polyhedron, 134(2017) 99-106.
39. N. Sarkar, M. Das, S. Chattopadhyay, Inorganica Chimica Acta, 457(2017) 19-28.
40. S. Kr Dey, A. Mukherjee, Coordination Chemistry Reviews, 310(2016) 80-115.
41. S. Thakur, N. Sarkar, M. G. B. Drew,A. Bauzá,A. Frontera, S. Chattopadhyay, Polyhedron, 142(2018) 83-92.
42. K. Ghosh, K. Harms, S. Chattopadhyay, Polyhedron, 123(2017) 162-175.
43. K. Ghosh, S. Roy, A. Ghosh, A. Banerjee, A. Bauzá, A. Frontera, S. Chattopadhyay, Polyhedron, 112(2016) 6-17.
44. M. J. Frisch, G. W. Trucks, H. B. Schlegel, G. E. Scuseria, M. A. Robb, J. R. Cheeseman, G. Scalmani, V. Barone, B. Mennucci, G. A. Petersson, H. Nakatsuji, M. Caricato, X. Li, H. P. Hratchian, A. F. Izmaylov, J. Bloino, G. Zheng, J. L. Sonnenberg, M. Hada, M. Ehara, K. Toyota, R. Fukuda, J. Hasegawa, M. Ishida, T. Nakajima, Y. Honda, O. Kitao, H. Nakai, T. Vreven, J. A. Montgomery, Jr., J. E. Peralta, F. Ogliaro, M. Bearpark, J. J. Heyd, E. Brothers, K. N. Kudin, V. N. Staroverov, R. Kobayashi, J. Normand, K. Raghavachari, A. Rendell, J. C. Burant, S. S. Iyengar, J. Tomasi, M. Cossi, N. Rega, J. M. Millam, M. Klene, J. E. Knox, J. B. Cross, V. Bakken, C. Adamo, J. Jaramillo, R. Gomperts, R. E. Stratmann, O. Yazyev, A. J. Austin, R. Cammi, C. Pomelli, J. W. Ochterski, R. L. Martin, K. Morokuma, V. G. Zakrzewski, G. A. Voth, P. Salvador, J. J. Dannenberg, S. Dapprich, A. D. Daniels, Ö. Farkas, J. B. Foresman, J. V. Ortiz, J. Cioslowski, D. J. Fox, Gaussian 09 (Gaussian, Inc., Wallingford CT, 2009).
45. H. Eschirig, "The fundamentals of density functional theory", Inst. Solid State Mater. Res. Dresden Univ. Technol. Dresden, (2003) 204.
46. R. Touzani, A. Ramdani, S. El Kadiri, F. Gourand, Molecules, 4(11) (1999) M116.
47. S. Radi, Y. Toubi, N. Draoui, O. Feron, O. Riant, Letters in Drug Design & Discovery, 9(3) (2012) 305-309.
48. F. Malek, N. Draoui, O. Feron, S. Radi, Res. Chem. Intermed, 40(2)(2014) 681-687.
49. S. Radi, Y. Toubi, I. Hamdani, A. Hakkou, F. Souna, I. Himri, M. Bouakka, Res. J. Chem. Sci., 2(4) (2012) 40-44.
50. E.I. Solomon, U.M. Sundaram, T.E. Machonkin, Chem. Rev. 96 (1996) 2563–2605.
51. T. Klabunde, C. Eicken, J. C. Saccettini, B. Krebs, Nat. Struct. Biol. 5(12) (1998) 1084-1090.
52. A. Panja, N. C. Jana, P. Brandão, Molecular Catalysis, 449 (2018) 49-61.
53. C. Lee, C. Hill, N. Carolina, "Into a functional of the electron density ff", 37(2) (1988).
54. A. D. Becke, J. Chem. Phys. 98(2), 1372-1377 (1993).
55. A. D. Becke, J. Chem. Phys. 98(7), 5648-5652 (1993).